

# RSC Advances



This is an *Accepted Manuscript*, which has been through the Royal Society of Chemistry peer review process and has been accepted for publication.

*Accepted Manuscripts* are published online shortly after acceptance, before technical editing, formatting and proof reading. Using this free service, authors can make their results available to the community, in citable form, before we publish the edited article. This *Accepted Manuscript* will be replaced by the edited, formatted and paginated article as soon as this is available.

You can find more information about *Accepted Manuscripts* in the [Information for Authors](#).

Please note that technical editing may introduce minor changes to the text and/or graphics, which may alter content. The journal's standard [Terms & Conditions](#) and the [Ethical guidelines](#) still apply. In no event shall the Royal Society of Chemistry be held responsible for any errors or omissions in this *Accepted Manuscript* or any consequences arising from the use of any information it contains.

## ARTICLE

## Screening of $\beta$ -hairpin peptide-engrafted 1,2,3-triazoles to identify APEH enzyme inhibitors

Cite this: DOI: 10.1039/x0xx00000x

A. Sandomenico<sup>1,2,\*†</sup>, V. Celentano<sup>1†</sup>, L. D. D'Andrea<sup>1,2</sup>, G. Palmieri<sup>3</sup>, M. Ruvo<sup>1,2\*</sup>

Received 00th January 2012,  
Accepted 00th January 2012

DOI: 10.1039/x0xx00000x

[www.rsc.org/](http://www.rsc.org/)

APEH catalyses the removal of N-terminal acetylated amino acids from proteins destined to degradation and is now recognized as a new therapeutic target for several diseases. New APEH inhibitors having triazole-based structures have been recently reported. On this basis we have screened a set of click-generated cyclic peptides, previously investigated for peptide conformational stability studies, as possible novel enzyme inhibitors. We find a clicked peptide, NHB3.3, that inhibits APEH activity and structure-activity studies highlighted that APEH inhibition is mediated by the spatial organization of the triazole ring and by its orientation and distance from the peptide scaffold, whose structural integrity, in turn, also plays a relevant role. In conclusion, our findings confirm that 1,2,3 triazoles are privileged pharmacophores for specific serine protease inhibitors and provide structural insights exploitable for modulating its inhibition activity.

**Keywords:** APEH; click-chemistry;  $\beta$ -hairpin peptide; serine-protease

### Introduction

APEH (EC 3.4.19.1), namely acyl-amino-acid-releasing enzyme (or acylpeptide hydrolase or acyl-amino-acyl peptide hydrolase), is a relatively new member of the prolyl oligopeptidase (POP) family of serine peptidases (clan SC, family S9)<sup>1</sup>. As most of enzymes belonging to the POP family, APEH hydrolyses short peptide substrates and present a canonical  $\alpha/\beta$  hydrolase fold, together with the Ser-Asp-His catalytic triad covered by an unusual  $\beta$ -propeller<sup>2</sup>. So far, this class of enzymes has been mainly found in a number of eukaryal and Archaea organisms as well as in a psychrotolerant bacterium<sup>3,4</sup>. APEH catalyses the removal of acetyl-amino acids from the N-terminus of short peptides and cytoplasmic proteins. For these properties the enzyme is attracting a vast attention for the potential role it can play in the complex mechanisms regulating protein turnover. Although the physiological role of APEH in cells is still unclear, several experimental evidences have highlighted the impact the activity of this enzyme may have on the fate of cancer cells.

Several reports have indeed suggested its implication in the molecular mechanisms of protein degradation<sup>5,6</sup> and its function as secondary antioxidant defence system against proteins

damaged by oxidative stress<sup>7</sup> and as modulator of cancer progression<sup>8-12</sup>.

The identification of potent and selective APEH inhibitors, for these reasons, is therefore become an important focus, because they serve as tools to investigate the enzyme downstream effects and may be employed in those therapeutic applications requiring a down-regulation of APEH activity<sup>7</sup>. Previously, we identified APEH inhibitors by screening a set of synthetic peptides designed on the reactive-site loop (RSL) of an APEH protein inhibitor<sup>6</sup>. A competitive inhibitor ( $K_i = 1.00 \pm 0.02 \mu\text{M}$ ) was derived from the first endogenous inhibitor SSCEi (Sulfolobus Solfataricus Chymotrypsin-Elastase inhibitor), and was employed to investigate the APEH role in the protein degradation machinery and its correlation with the UPS (ubiquitin-proteasome-system). By screening a random peptide library<sup>13</sup> we also selected a modified tetrapeptide, named CF<sub>3</sub>-Imph, showing an unusual uncompetitive inhibition activity. CF<sub>3</sub>-Imph was able to block the APEH activity in cells without significant effect on cell proliferation and caspase activity<sup>13</sup>. The different effects produced by the two APEH inhibitors on cells proliferation, suggested a possible intriguing relationship between the mechanism of APEH inhibition and proteasome activity. Recently, 1,2,3-triazole urea-derivatives

have also been identified as potent inhibitors of APEH and other serine hydrolases<sup>14</sup>. On this basis, we have reasoned that click-generated peptide-grafted triazoles could inhibit the enzyme and that peptide sequence and structure might modulate such activity. To test this hypothesis we screened a set of 1,4-disubstituted 1,2,3-triazole engrafted on a modified Trpzip2 peptide scaffold previously generated for peptide conformational stability studies<sup>15</sup>. These compounds consisted of a triazole ring attached to a peptide chain through the spacers provided by the side chains of different precursors. For this purpose, we used azide- and propargyl-bearing residues in which the number and position of methylene units were varied (Figure S1). After screening the first set of molecules, we prepared and tested new analogues to dissect the relative contribution of the different molecular substructures to APEH recognition and inhibition. The best inhibitor has then been characterized in terms of specificity and mechanism of inhibition toward APEH.

## Results and discussion

### Library Preparation and Characterization

All crude peptidomimetics were obtained with average yields of 50-70% and after RP-HPLC purification homogeneous products were isolated. Experimental molecular masses were all consistent with the expected values (Table S1). Unprotected linear peptides were cyclized (clicked) via a CuAAC reaction as described in the Methods; since the triazole ring formation does not involve a change of the molecular weight, cyclization was monitored via RP-HPLC by the formation of products with significantly shorter retention times compared to the corresponding linear products and with the same molecular masses<sup>15</sup> (Table S1). Conversions were all quantitative. The NHB3.3<sub>open</sub> peptide was obtained by treatment with trypsin of the NHB3.3 cyclic precursor. This treatment afforded only one HPLC peak with a mass corresponding to the open hydrolyzed peptide. The cleaved peptide was purified to homogeneity by RP-HPLC.

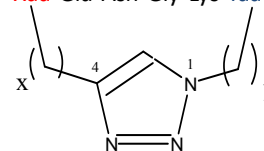
### Screening of clicked peptidomimetics

#### Screening of the 1st generation library of NHB peptides

With the 1st generation library of NHB peptidomimetics (Figure 1, entries 1-15; Figure S2 and S3) we tested the hypothesis that 1,2,3-triazole-containing molecules could work as APEH inhibitors and that the activity could depend on the specific orientation and flexibility of the triazole-containing linker imposed by the size of the cycle generated after the click reaction. The ability of these peptidomimetics to inhibit APEH activity was tested in a biochemical assay utilizing the specific substrate N-acetyl-L-alanine *p*-nitroanilide (AANA). Peptidomimetics concentrations were determined by UV spectroscopy; the screening was performed at a concentration of 25  $\mu$ M. As shown in Figure 2A, the screening revealed that only the molecule named NHB3.3, containing three methylene groups on both linkers connecting the triazole ring to the peptide chain, showed a relevant ability to inhibit APEH,

indeed more than 80% activity suppression was observed with this compound used at 25  $\mu$ M.

Ser-Trp-Thr-Xaa-Glu-Asn-Gly-Lys-Yaa-Thr-Val-Lys-NH<sub>2</sub>



N°	Name	Xaa	Yaa	x	y
1	NHB 1.1	Pra	Dap(N3)	1	1
2	NHB 1.2	Pra	Dab(N3)	1	2
3	NHB 1.3	Pra	Orn(N3)	1	3
4	NHB 1.4	Pra	Lys(N3)	1	4
5	NHB 2.1	Hpg	Dap(N3)	2	1
6	NHB 2.2	Hpg	Dab(N3)	2	2
7	NHB 2.3	Hpg	Orn(N3)	2	3
8	NHB 2.4	Hpg	Lys(N3)	2	4
9	NHB 3.1	Bpg	Dap(N3)	3	1
10	NHB 3.2	Bpg	Dab(N3)	3	2
11	NHB 3.3	Bpg	Orn(N3)	3	3
12	NHB 3.4	Bpg	Lys(N3)	3	4
13	NHB 1.2 rev	Dap(N3)	Hpg	1	2
14	NHB 2.1.rev	Dab(N3)	Pra	2	1
15	NHB 2.1 W3	Hpg	Dap(N3)	2	1
16	NHB 3.3_C	Bpg	Orn(N3)	3	3
17	NHB 3.3_N	Bpg	Orn(N3)	3	3
18	NHB 3.3_CN	Bpg	Orn(N3)	3	3
19	NHB 3.3 $\Delta$ tum	Bpg	Orn(N3)	3	3
20	NHB 3.3 open	Bpg	Orn(N3)	3	3

**Figure 1:** Top: generic molecular structure of the 1st generation library (entries 1-15) of NHB clicked peptidomimetics. Bottom: Nomenclature used to identify the tested compounds; x and y indicate the number of methylene groups on the 1,4-disubstituted 1,2,3-derived cyclic molecules. Detailed molecular structures of all compounds are reported as supplementary material.

Two additional compounds, NHB1.2 and NHB1.2rev, exhibited a significant inhibition, but they reduced APEH activity for only 40% and 30%, respectively. Next, a dose-response assay was carried out using NHB3.3 at increasing concentrations between 0 and 30  $\mu$ M. As reported in Figure 2B, APEH inhibition followed a hyperbolic trend, reaching 80% at the highest inhibitor concentration. The extrapolated IC<sub>50</sub> was 10.5  $\pm$  1.7\*10<sup>-6</sup> M. Remarkably, the NHB3.3 unclicked linear variant, lacking of the triazole ring, when tested at 10  $\mu$ M, 25  $\mu$ M and 100  $\mu$ M, exhibited only a poor inhibition (13.2%, 16.4% and 22.6%, respectively; Figure 2C) confirming the critical role exerted by the 1,2,3-triazole moiety in blocking APEH activity<sup>14</sup>. In addition, the very poor activity displayed by other library components bearing the triazole ring, demonstrated that inhibition of APEH by NHB3.3 also depends on specific structural properties beyond the presence of the heterocycle. Data thus suggest that the specific peptide

structure, the triazole moiety and, more importantly, the spatial orientation induced by the length of 1,4 substituents, together contribute to the inhibiting activity toward APEH.

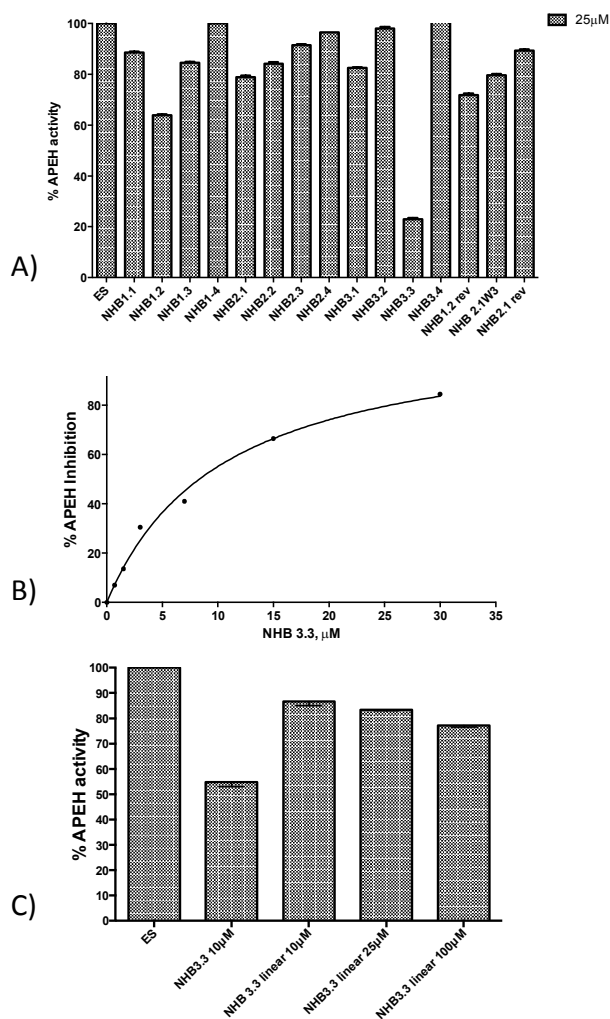


**Figure 2:** A) Inhibition of APEH activity by clicked peptidomimetics included the 1th generation library of NHB compounds. Peptides were tested at the concentration of 25 μM. B) Dose-response assay for the most active compound. The  $IC_{50}$  value ( $10.5 \pm 1.7 \times 10^{-6}$  M) was determined by fitting the experimental data with the GraphPad Prism software, using a nonlinear curve-fitting method and a simple binding isotherm equation  $\{\% I = \% I_{max} * [I]/(IC_{50} + [I])\}$ . C) Inhibition of APEH activity by clicked NHB3.3 and its corresponding unclicked (linear) precursor tested at the concentration of 10, 25 and 100 μM.

#### Screening of the 2nd generation NHB library

The library of 2nd generation NHB-clicked peptidomimetics (entries 16-20 in Figure 1, Figure S3) was screened at 10 μM, using as reference NHB3.3 at the same concentration. As shown in **Figure 3**, all three shortened NHB3.3 variants, NHB3.3\_C, NHB3.3\_N, and NHB3.3\_NC, blocked APEH activity only up to about 25%, which is much less compared to 50% exhibited by NHB3.3 at the same concentration. This further supported the notion that the structural integrity of the NHB peptidomimetic is strongly required for the most efficient enzyme recognition and inhibition. Strikingly, the linear

unclicked variants of all 3 compounds were significantly less active, confirming the need for the triazole ring for inhibition. For a better comparison of the shortened NHB3.3 variants efficacy, we next carried out dose-response assays (**Figure 4A-C**). The three peptides suppressed APEH activity by only 35% at the highest concentration used (150 μM), which is by far lower compared to 80% inhibition displayed by NHB3.3 at 30 μM.

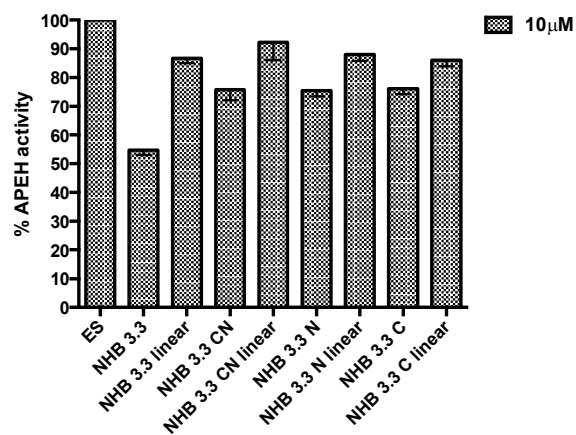


**Figure 3:** Inhibition of APEH activity by the set of 2nd generation of NHB3.3 peptidomimetics and the corresponding unclicked linear variants tested at 10 μM.

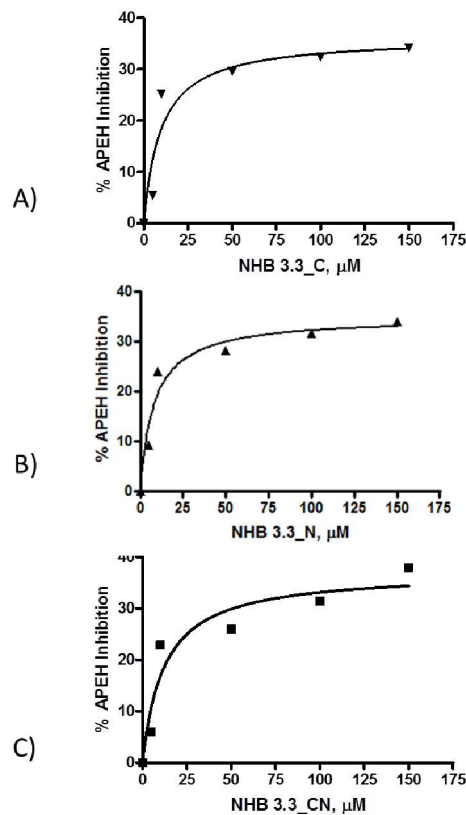


**Figure 4:** Dose-response assay for NHB3.3\_C (A) NHB3.3\_N (B) and NHB3.3\_CN (C) carried out at concentrations between 5 and 150 μM.

### Mechanism of inhibition

To further investigate the role played by the peptide structure in APEH inhibition, we generated and tested the acyclic variants NHB3.3\_Δturn and NHB 3.3\_open. We found that both the absence of the β-turn sequence and splitting of the molecule on the internal lysine, negatively affected the peptide activity, which, at the maximum concentration of 100 μM, was 21% and 31% (Figure 5A), respectively. NHB3.3\_open was also dose-dependently tested at concentrations between 0 and 200 μM, confirming that less than 30% inhibition was afforded by this compound, even at very high concentrations (Figure 5B). To assess the role of the N-terminal free amino group, we finally tested the activity of the acetylated NHB3.3 variant (NHB3.3Ac). Strikingly, capping the free amino group completely ablated the inhibition properties, suggesting a direct involvement of this group in enzyme recognition or a strong influence of the peptide net charge (Figure 6).

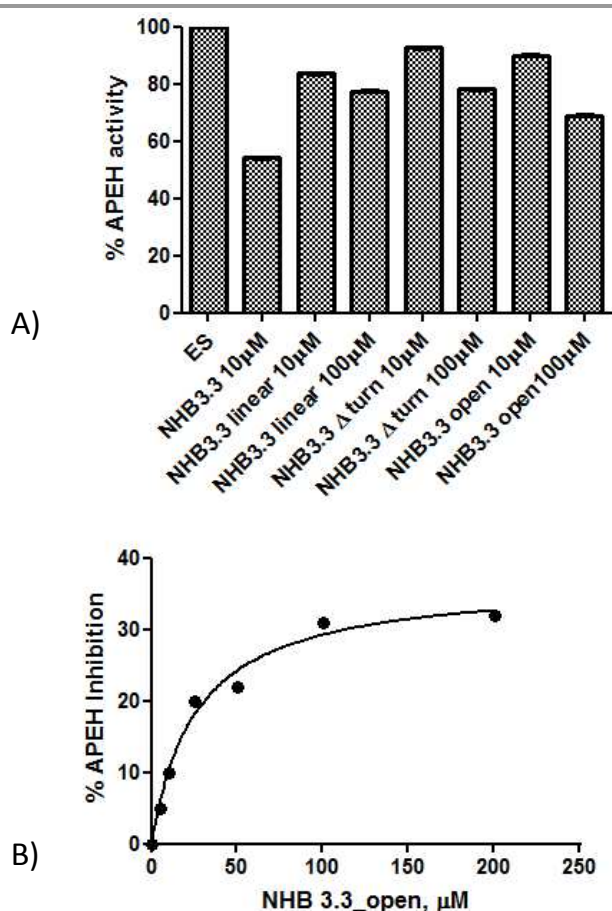


**Figure 5:** A) Inhibition of APEH activity by NHB3.3\_Δturn and NHB3.3\_open at 10 μM and 100 μM. B) Dose-response assays for NHB3.3\_open carried out at concentrations between 5-200 μM

To further gain insights into the recognition, we explored the inhibition mechanism of NHB3.3 toward APEH purified from porcine liver. The enzyme was pre-incubated with the inhibitor at two concentrations and the residual enzymatic activity was

assessed in the presence of increasing concentrations of the AANA substrate. The Lineweaver–Burk plots where the y-intercept is equivalent to the inverse of  $V_{max}$  and the x-intercept represents  $-1/K_m$ , reported in Figure 7A, shows that the lines obtained at different inhibitor concentrations, do not intersect on the  $1/V_{max}$  axis, suggesting that the compound acts as a non-competitive inhibitor. The inhibition constants  $K_i$  was estimated by the Lineweaver–Burk equation (Figure 7B), which provided a value of  $10.8 \pm 3.7 \cdot 10^{-6}$  M, in close agreement with the  $IC_{50}$  value obtained in the dose-response inhibition assay. Also a  $K_m$  of 100 μM could be determined by this approach.

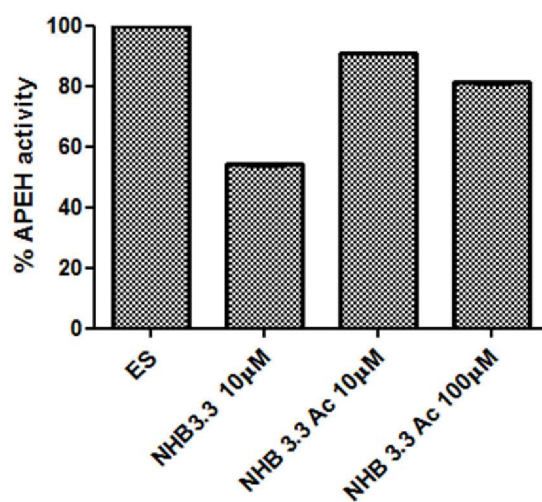


**Figure 6:** Inhibition of APEH activity by acetylated NHB3.3 variants tested at the concentrations of 10 μM and 100 μM.

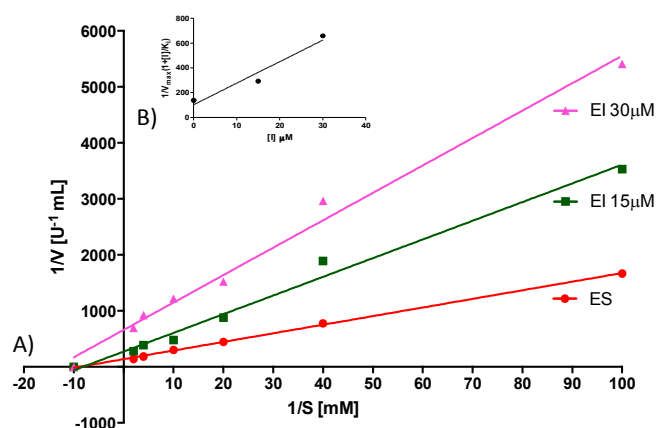


**Figure 7:** A) Inhibition kinetic analysis. APEH was incubated without (ES) or with the NHB3.3 at 15 μM (EI 15 μM) and 30 μM (EI 30 μM) and assayed at increasing concentrations of substrate (5-500 μM). The reciprocals of the rate of the substrate hydrolysis for each inhibitor concentration were plotted against the reciprocals of the substrate concentrations. B) By a plot of  $(1 + I/K_i)$  against the NHB3.3 concentration a dissociation constant ( $K_i$ ) value was extrapolated which is consistent with the  $IC_{50}$  determined previously.

### Inhibition specificity

We next determined the NHB3.3 specificity toward APEH. The activity of the peptide inhibitor was thus probed against a panel of serine proteases, including elastase, trypsin, chymotrypsin and subtilisin. The chymotrypsin-like activity of proteasome was also probed using a suitable chromogenic substrate. Results are summarized in **Table 1**.

The triazole-peptide was inactive toward trypsin, elastase and subtilisin, whereas it inhibited chymotrypsin by 30% and proteasome by 45% at 50  $\mu\text{M}$ , a concentration sufficient to completely abolish APEH activity (**Table 1**). Data are thus suggestive of a strong ability of the inhibitor to discriminate between APEH and other proteases showing similar mechanisms, though it is capable to partially interfere with the chymotrypsin activity shared by chymotrypsin itself and one of the proteasome subunits ( $\beta 5$ ).

**Table 1** Inhibition activity of NHB3.3 toward a set of serine proteases. APEH is included as a reference. Data were generated as described in the Methods.

	100 $\mu\text{M}$	50 $\mu\text{M}$	25 $\mu\text{M}$
Trypsin	No inhibition	No inhibition	No inhibition
Elastase	No inhibition	No inhibition	No inhibition
Subtilisin	No inhibition	No inhibition	No inhibition
Chymotrypsin	60%	30%	15%
Proteasome	63%	45%	30%
APEH	100%	100%	80%

### Discussion

In this study, we have screened a set of click-generated triazole-containing cyclic peptidomimetic to select inhibitors of the enzyme APEH, which is now recognized as a new therapeutic target for several diseases, including cardiovascular diseases, cancer, inflammation, haematological diseases, neurological and urological diseases.<sup>[3]</sup> All the clicked compounds have a common Trpzip2-like peptide structure, whereas the linkers connecting the peptide to the triazole ring varied in length affecting the  $\beta$ -hairpin conformational stability<sup>15</sup>. We selected the NHB3.3 clicked peptide as the best APEH inhibitor among all the tested analogues. NHB3.3 bears on both  $\beta$ -hairpin strands three methylene groups deriving from the triazole precursors bis-homopropargylglycine (Bpg) and L- $\delta$ -azidoornitine (Orn(N3)). NHB3.3 dose-dependently blunts APEH activity with an 80% maximum inhibition reached at 30  $\mu\text{M}$  and with an  $\text{IC}_{50}$  of  $10.5 \pm 1.7$   $\mu\text{M}$ . Remarkably, enzyme inhibition occurs through a non-competitive mechanism, therefore enzyme recognition likely takes place on a site not overlapped with the catalytic pocket and could involve an allosteric mechanism. Our findings are in agreement with previous data by Adibekian *et al.*<sup>14</sup> showing that APEH is inhibited by substituted 1,2,3-triazoles. Compared to N-heterocyclic ureas triazole-based inhibitors, which have subnanomolar activities<sup>14</sup>, our inhibitor shows a much lower inhibition efficiency. It should be underscored that irreversible hydrolase inhibitors do interact covalently with the target enzyme, showing tremendously high potencies. However, while

potency is undoubtedly the most important aspect, it should be considered that they are not generally well accepted for eventual clinical use, especially when the target biology is still controversial and not well understood as in the case of APEH. We therefore believe that reversible inhibitors, as those potentially obtainable from those we report here, would be invaluable tools to further investigate the therapeutic potential of APEH.

A step forward in the process of improving our inhibitors' potency will be the introduction of a second recognition center, which would ideally synergize with the triazole primary unit to interact with and reversibly block the enzyme<sup>14,16</sup>. The peptide structure of NHB3.3 may serve for this purpose, acting as a support for introducing such auxiliary anchoring point. In this instance it should be underscored that the peptide structure and the triazole moiety together contribute to enzyme recognition and inhibition, therefore the site for modification must be carefully chosen. Our structure-activity relationship study on NHB3.3 has indeed confirmed that the intact triazole ring and a specific spatial orientation are both required for activity. The peptide structure clearly functions as a scaffold for properly positioning the ring, therefore the secondary structure has a primary importance for this purpose.

As reported by Celentano *et al.*<sup>15</sup>, NHB3.3 adopts a  $\beta$ -hairpin structure, but among those studied at structural level, it is not the one with the highest  $\beta$ -hairpin content. On the other hand, the peptide NHB2.1, which showed the highest  $\beta$ -hairpin content<sup>15</sup>, only moderately (around 20%) affects APEH activity. This suggests that the conformational stability of the peptide  $\beta$ -hairpin structure is not a requirement for activity, rather a partial flexibility seems to favour enzyme recognition. Indeed, increasing the linker length (NHB3.4 vs NHB3.3) the peptide inhibitory activity is completely abolished, suggesting that the size of the bridge supporting the triazole ring could be critical. It has to be noted that peptides with four methylene groups are always the worst inhibitor for each NHB series with a fixed x number (i.e. NHB1.1, NHB1.2, NHB1.3, NHB1.4).

Fixed the optimal orientation between the triazole ring and the peptide chain (such as in NHB3.3), it seems that the structural integrity of the  $\beta$ -hairpin also plays a role in APEH inhibition. Removal of the turn residues (NHB3.3\_ $\Delta$ turn), turn opening (NHB3.3\_open), deletion of peptide termini (NHB3.3\_N, NHB3.3\_C or NHB3.3\_NC) renders NHB3.3 ineffective or reduces APEH inhibition. It is therefore reasonable to hypothesize that these backbone modifications abolish the inhibition activity, by drastically modifying the  $\beta$ -hairpin secondary structure.

Taken together these experimental observations confirm that the inhibitory effect of peptide NHB3.3 depends on the spatial organization of the triazole ring, its orientation and distance with respect to the peptide chain and on the structural integrity of the peptide scaffold

### Conclusions

In conclusion, our findings confirm that 1,2,3-triazoles are key components of a pharmacophoric structure common to serine

protease and more specifically APEH inhibitors and that such structural module is exploitable to finely regulate the inhibition activity. Given the increasing importance of APEH in several diseases and its connection with the molecular mechanisms of protein turnover, peptide-linked 1,2,3-triazole derivatives can represent versatile tools for developing more potent and specific APEH-inhibitors.

## Experimental

### Materials

Protected amino acids for the synthesis of peptides and the activators N-hydroxybenzotriazole (HOBT) and O-benzotriazole-N,N,N',N'-tetramethyl-uronium-hexafluoro-phosphate (HBTU) coupling agents were from Merck except Fmoc-L-Dap(N3)-OH, Fmoc-L-Dab(N3)-OH, Fmoc-L-Orn(N3)-OH which were from Iris Biotech GmbH. Solvents for peptide synthesis and purification, acetic anhydride, Ascorbic acid and Copper(II) sulfate pentahydrate were from Sigma-Aldrich (Milan, Italy). Piperidine was purchased from Biosolve; N,N-diisopropylethylamine (DIPEA) was provided by Romil. Porcine liver APEH was obtained from Takara BIO INC. (Shiga Japan). Acetyl-Ala-pNA was from Bachem (Laufelfingen, Switzerland). Elastase, Subtilisin, Trypsin, and Chymotrypsin were from Sigma-Aldrich (Milano, Italy). Purified human erythrocyte proteasome was from Boston Biochem (Boston, USA). N-Succinyl-Ala-Ala-Pro-Phe p-nitroanilide (Suc-AAPF-pNA). N $\alpha$ -Benzoyl-L-arginine 4-nitroanilide hydrochloride (L-BAPA) and N-Succinyl-Leu-Leu-Val-Tyr-7-Amido-4-Methylcoumarin substrate were from Sigma-Aldrich (Milano, Italy).

### Library Preparation and Characterization

Given the occurrence of 1,2,3-triazole moieties in small molecule inhibitors of APEH<sup>14</sup>, we have initially used a series of available short peptides side chain cyclized via Cu(I)-catalyzed azide alkyne cycloaddition (CuAAC) reactions. After the click reaction, compounds incorporated a 1,4-disubstituted 1,2,3-triazole-ring engrafted on a Trpzip2-derived peptide scaffold<sup>15</sup> in which two residues in non-hydrogen bonded (NHB) positions, Trp4 and Trp9, were replaced with a homologue series of alkyne and azide amino acids. The basic structures of the click peptides used in this study and the molecular formulas of the unnatural amino acids used are reported in Figure S1, S2 and S3 supplied as supplementary material.

Unnatural amino acids with different side chain lengths were introduced on the Xaa and Yaa positions. Specifically, on position Xaa we introduced alkyne propargylglycine (Pra), homopropargylglycine (Hpg), bishomopropargylglycine (Bpg), while in position Yaa we placed L- $\beta$ -azidoalanine (Dap (N3)), L- $\gamma$ -azido-homoalanine (Dab (N3)), L- $\delta$ -azido-orntine (Orn (N3)) and N- $\epsilon$ -Azido-L-lysine (Lys (N3)). The different combinations of Xaa and Yaa are reported in Figure 1 and Figure S1. The first group of resulting 12 click compounds were named 1<sup>th</sup> generation library of NHB-clicked peptides. To further investigate the inhibition properties of this class of compounds, we also screened in the same set three additional peptides, named NHB1.2rev, NHB2.1rev and NHB-W3<sup>15</sup>. In NHB1.2rev and NHB2.1rev, the positions of alkyne-

and azide- amino acids were exchanged compared to the NHB1.2 and NHB2.1 parent peptides (Figure 1 and Figure S2 and S3), peptides from number 1 to 15), while in NHB-W3 the tryptophan originally on position 2, was placed on position 3. To investigate the influence of selected residues from the Trpzip2-like peptide sequence on APEH recognition and inhibition, after the screening of the first generation library, we designed and synthesized a second set of NHB3.3-derived compounds (2<sup>nd</sup> generation of NHB-clicked peptides (Figure 1 and Figure S3) peptides from number 16 to 20). In particular, we generated the unclicked linear variant (NHB3.3\_linear), and three chain shortened peptide variants where the C-terminal Threonine, Valine and Lysine (NHB3.3\_C), the N-terminal Serine and Threonine (3.3\_N) or both (NHB3.3\_NC) were ablated. Tryptophan was maintained in all compounds to perform UV quantification. We also designed and synthesized a non-cyclic NHB3.3 variant without the internal  $\beta$ -turn sequence Glu-Asn-Gly-Lys (NHB3.3\_ $\Delta$ turn). An additional ring open variant of clicked NHB3.3 was obtained by splitting the bond between Lysine and Orn(N3) with trypsin (NHB3.3\_open).

All peptides were synthesized on solid phase by standard Fmoc chemistry using a Rink Amide MBHA resin (0.54 mmol/g substitution) as solid support, as it releases peptides amidated at C-terminus upon acid treatment. All couplings were performed twice for 20 min by using an excess (2.5 equivalent) of each amino acid derivative. Amino acids were activated in situ by 2.49 equivalents of HOBT/HBTU and 5 equivalents of DIPEA. Fmoc deprotection was performed with 30% piperidine in DMF (5 min, twice). After the last coupling, unreacted N-terminal amino groups were acetylated with a solution of 2.0 M Acetic Anhydride, 0.06 M HOBT, 0.55 M DIPEA in NMP (5 min.). Peptide cleavage from the solid support and simultaneous removal of all protecting groups from amino acid side chains was carried out by suspending the fully protected compound-resins in a TFA/H<sub>2</sub>O/TIS (95:2.5:2.5) mixture for 3 h. Crude products were precipitated by addition of cold diethyl ether after filtration of the resin, washed three times with diethyl ether, collected by centrifugation, dissolved in a water/acetonitrile mixture and lyophilized. The purified linear peptides were subjected to cyclization by Cu(I)-catalyzed azide alkyne cycloaddition (CuAAC) reaction (0.5 mM peptide, 7 mM CuSO<sub>4</sub>, 6.5 mM ascorbic acid in H<sub>2</sub>O/CH<sub>3</sub>OH (2:1 V/V)) at r.t. for 60 min<sup>17-19</sup>. Analytical RP-HPLC runs were carried out on an HP Agilent Series 1200 chromatograph using a Proteo C12 column (4  $\mu$ m, 90  $\text{\AA}$ , 4.6x250 mm (Phenomenex, Torrance, CA) operated at a flow rate of 1.0 mL/min. Preparative RP-HPLC was carried out on a Shimadzu 8A chromatograph coupled with an UV detector, using an AXIA column 50x21.2 mm, 4 $\mu$ m (Phenomenex, Torrance, CA); the flow rate was 20 mL/min. For all the RP-HPLC purifications the system solvent used was: H<sub>2</sub>O 0.1% TFA (solvent A) and CH<sub>3</sub>CN 0.1% TFA (solvent B). Typical linear gradients starting from 5% to 70% B in 20 min were applied; UV detectors were set at 210 nm and 280 nm. The purified clicked peptides were characterized by LC-MS using an LCQ DECA XP Ion Trap mass spectrometer equipped with an OPTON ESI source, operating at 4.2 kV needle voltage and 320  $^{\circ}$ C and coupled to a complete Surveyor HPLC system, comprising an MS pump, an autosampler and a photo diode array (PDA) detector. A Jupiter C18 column (5  $\mu$ m, 300A, 250x2 mm, Phenomenex) at a flow rate 0.2

mL/min was used in these analyses. Typical LC-MS gradients were from 5% to 70% solvent B (acetonitrile with added 0.05% TFA; solvent A was water with 0.05% TFA). NHB3.3<sub>open</sub> was obtained by tryptic digestion. The reaction was carried out adding porcine trypsin at 1:10 w/w in 50 mM Tris-HCl pH 7.5 for 4h at 37° C. The reaction was stopped by acidification with H<sub>2</sub>O, 0.1% TFA. The product was analysed by LC-MS and purified to homogeneity as described above for the other compounds.

### Screening of clicked peptides

The screening was carried out by a spectrophotometric assay using porcine Acyl peptide hydrolase (APEH) enzyme and the synthetic specific substrate N-acetyl-L-alanine *p*-nitroanilide (AANA). The reaction mixture (0.2 mL), containing pure APEH (0.5 nM) in 50 mM Tris-HCl buffer pH 7.5, was pre-incubated at 37 °C for 2 min. Then, 16 μM AANA was added. The release of *p*-nitroanilide ( $\epsilon = 8800 \text{ M}^{-1} \text{ cm}^{-1}$ ) was measured by recording the absorbance increase at 410 nm on a Synergy multi-wavelength plate reader (Biotek), equipped with a thermostated compartment. Assays were performed in triplicates in 96-well polyethylene plates. The inhibition screening assay was carried out by pre-incubating each peptide (25 μM) with the enzyme for 10 min at 37 °C prior addition of the substrate. The absorbance at 410 nm was continuously monitored in each well and the slope of each straight line was obtained. Data were processed by averaging replicate values and calculating slopes by linear regression analysis. The inhibition extents (%) were determined by comparing the slopes obtained from inhibition assays with those resulting from control experiment (assumed 100%).

Dose-response assays with NHB3.3 were performed at concentrations ranging between 0.7 and 30 μM with the purpose of confirming results at different concentrations and to determine IC<sub>50</sub>. The 2<sup>nd</sup> generation of NHB-clicked peptides, including both the  $\Delta$ turn and open variants, was dose-dependently screened at concentrations between 10 μM and 100 μM.

Dose-dependent assays were also conducted for NHB3.3<sub>C</sub>, NHB3.3<sub>N</sub> and NHB3.3<sub>NC</sub> at concentrations between 5 μM and 150 μM. IC<sub>50</sub> values were extrapolated by data fitting with the GraphPad Prism software by using a nonlinear curve-fitting method and a simple binding isotherm equation  $\{\% I = \% I_{\text{max}} * [I]/(IC_{50} + [I])\}$ . All assays were performed in 96-well plates and each data point was determined as triplicate. Experiments were repeated at least two times. Data are reported as values  $\pm$  standard deviation.

### Mechanism of Inhibition

To determine the mechanism of enzyme inhibition, APEH (0.5 nM) was pre-incubated without and with NHB3.3 at 15 μM and 30 μM and its activity was tested at increasing substrate concentrations (between 5 and 500 μM). For each inhibitor concentration, a Lineweaver-Burk double reciprocal plot was built by plotting the reciprocal of substrate hydrolysis rate as a function of the reciprocals of substrate concentrations. The inhibition constant  $K_i$  was determined by the Lineweaver-Burk equation  $\{1/V = (K_m/V_{\text{max}})*(1 + I/K_i) * 1/S + 1/V_{\text{max}} * (1 + I/K_i)\}$ .

### Inhibition specificity

To assess the specificity of NHB3.3 in inhibiting APEH, we tested its activity against a panel of other common serine proteases. For this purpose we used elastase, subtilisin, trypsin, chymotrypsin and proteasome with the suitable chromogenic substrates. For proteasome the chymotrypsin-like activity was probed. Reactions were performed in 1 mL of buffer. For elastase, subtilisin, trypsin, chymotrypsin and APEH, assays were performed using the specific chromogenic substrates reported below, all having a *p*-nitroanilide reporter (pNA). Enzymatic activities were measured on a Cary 100 Scan (Varian) UV/Vis spectrophotometer, equipped with a thermostated cuvette compartment by recording the absorbance increase at 410 nm due to *p*-nitroaniline release. The chymotrypsin-like activity of proteasome was determined by a fluorimetric assay where the reporter was amido-4-methylcoumarin. In detail, elastase and subtilisin activities were determined using a 400 nM solution of enzyme in 25 mM Tris-HCl pH 8.0 and 100 μM Suc-AAPF-pNA substrate. Trypsin was assayed using the enzyme at 160 nM in 50 mM Tris-HCl buffer pH 8.0 containing 20 mM CaCl<sub>2</sub> and 100 μM L-BAPA substrate. Chymotrypsin activity was tested using the enzyme at 50 nM in 50 mM Tris-HCl buffer pH 8.0 containing 20 mM CaCl<sub>2</sub> and 100 μM Suc-AAPF-pNA substrate. The chymotrypsin-like activity of proteasome (170 nM) was measured in 25 mM Tris-HCl pH 7.5 using 50 μM of N-Succinyl-Leu-Leu-Val-Tyr-7-amido-4-methylcoumarin substrate. The enzymatic activity was monitored on a Cary 100 Scan (Varian) UV/Vis spectrofluorimeter, equipped with a thermostated cuvette compartment using as excitation wavelength 345 nm and as emission wavelength 445 nm. Protease inhibiting activities were carried out using a fixed amount of enzymes and increasing peptide concentrations (25, 50 and 100 μM). Mixtures were pre-incubated for 30 min at 37 °C before the addition of the substrate, and the enzymatic activities were followed as described above. Experiments were repeated at least three times.

### Acknowledgements

This work was supported by funds from FIRB MERIT N° RBNE08NKH7\_003 and from PON Ricerca e Competitivita 2007-2013 (PON01\_01602, PON01\_02342) to MR. AS is fully supported by FIRB N° RBNE08NKH7\_003.

### Conflict of interest

The authors declare no financial or commercial conflict of interest.

### ABBREVIATIONS

DMF: Dimethylformamide  
DCM: Dichloromethane  
DIEA: N,N-Diisopropylethylamine  
HBTU: O-Benzotriazole-N,N,N',N'-tetramethyluronium-hexafluoro-phosphate  
HOBt: N-hydroxybenzotriazole  
HPLC: High Performance Liquid Chromatography



LC-MS: Liquid Chromatography Mass Spectrometry

NHB: Non-Hydrogen Bonded

TIS: Tri-isopropylsilane

TFA: Trifluoroacetic acid

## Notes and references

<sup>1</sup> Institute of Biostructure and Bioimaging, National Research Council (CNR-IBB), Naples, Italy.

<sup>2</sup> CIRPEB - University of Naples Federico II, Naples, Italy

<sup>3</sup> Institute of Biosciences and BioResources, National Research Council (CNR-IBBR), Naples, Italy.

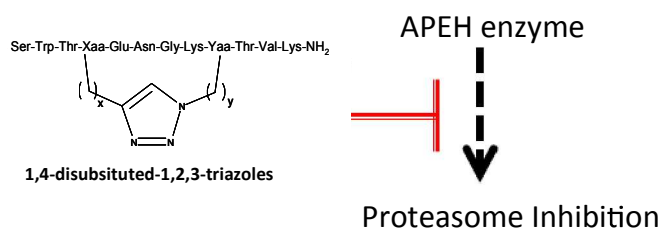
†These authors equally contributed to this work.

\*Correspondence: Dr. Annamaria Sandomenico and Dr. Menotti Ruvo, Institute of Biostructure and Bioimaging, National Research Council (CNR-IBB), and CIRPeB, Via Mezzocannone 16, 80134 Naples, Italy.

Email: annamaria.sandomenico@gmail.com; menotti.ruvo@unina.it

Phone: 0039-081-2536644; Fax: 0039-081-2534574.

**Table of contents entry:** Peptide-grafted triazoles, obtained via click chemistry, drive the inhibition activity toward Acyl Peptide Hydrolase (APEH), a modulator of the proteasome activity.



## References

- [1] Szeltner, Z., Rea, D., Juhász, T., Renner, V., Fülöp, V., Polgár, L. *J. Mol. Biol.* 2004, **340**, 627.
- [2] Rea, D., Fülöp, V. *Cell Biochem. Biophys.* 2006, **44**, 349.
- [3] Sharma, K.K., Ortwerth, B.J. *Eur.J.Biochem.* 1993, **216**, 631.
- [4] Brunialti, E.A., Gatti-Lafranconi, P., Lotti, M. *Biochimie.* 2011, **93**, 1543.
- [5] Perrier, J., Durand, A., Giardina, T., Puigserver, A. 2005, **87**, 673.
- [6] Palmieri, G., Bergamo, P., Luini, A., Ruvo, M., Gogliettino, M., Langella, E., Saviano, M., Hegde R.N., Sandomenico, A., Rossi, M. *PLoS One* 2011, doi: 10.1371/journal.pone.0025888.
- [7] Shimizu, K., Fujino, T., Ando, K., Hayakawa, M., Yasuda, H., Kikugawa, K. *Biochem. Biophys. Res. Commun.* 2003, **304**, 766.
- [8] Scaloni, A., Jones, W., Pospischil, M., Sassa, S., Schneewind, O., Popowicz, A.M., Bossa, F., Graziano, S.L., Manning, J.M. *J. Lab. Clin. Med.* 1992, **120**, 546.
- [9] Erlandsson, R., Boldog, F., Persson, B., Zabarovsky, E.R., Allikmets, R.L., Sümegi, J., Klein, G., Jörnvall, H. *Oncogene* 1991, **6**, 1293.
- [10] Naylor, S.L., Marshall, A., Hensel, C., Martinez, P.F., Holley, B., Sakaguchi, A.Y. *Genomics* 1989, **4**, 355.
- [11] Yamaguchi, M., Kambayashi, D., Toda, J., Sano, T., Toyoshima, S., Hojo, H. *Biochem. Biophys. Res. Commun.* 1999, **263**, 139.
- [12] Bergamo, P., Cocca, E., Palumbo, R., Gogliettino, M., Rossi, M., Palmieri, G. *PLoS One* 2013, doi: 10.1371/journal.pone.0080900.

- [13] Sandomenico, A., Russo, A., Palmieri, G., Bergamo, P., Gogliettino, M., Falcigno, L., Ruvo, M. *J. Med. Chem.* 2012, **55**, 2102.
- [14] Adibekian, A., Martin, B.R., Wang, C., Hsu, K.L., Bachovchin, D.A., Niessen, S., Hoover, H., Cravatt, B.F. *Nat. Chem. Biol.* 2011, **7**, 469.
- [15] Celentano, V., Diana, D., De Rosa, L., Romanelli, A., Fattorusso, R., D'Andrea, L.D. *Chem. Commun. (Camb)* 2012, **48**, 762.
- [16] Ebdrup, S., Sorensen, L.G., Olsen, O.H. & Jacobsen, P. *J. Med. Chem.* 2004, **47**, 400.
- [17] Jagasia, R., Holub, J.M., Bollinger, M., Kirshenbaum, K., Finn, M.G. *J. Org. Chem.* 2009, **74**, 2964.
- [18] Tornøe, C. W., Christensen C. and Meldal, M., *J. Org. Chem.* 2002, **67**, 3057.
- [19] Li, H., Aneja, R., and Chaiken, I. *Molecules* 2013, **18**, 9797.